Periodica Polytechnica Mechanical Engineering

59(4), pp. 176-181, 2015
DOI: 10.3311/PPme.8298

RESEARCH ARTICLE

Friction Effects on Stability of a Digitally Controlled Pendulum

Csaba Budai[1*], László L. Kovács[2,3]

Received 02 June 2015; accepted after revision 13 August 2015

Abstract

This paper investigates the stability of a digitally controlled pendulum with Coulomb friction as primary source of dissipation. We focus on the stabilizing effect of friction against vibrations due to the otherwise unstable parameter settings, and we show how the stable domain of operation is expanded compared to the undamped case. Continuous time and discrete switched models are simulated to get information about the stabilization effect of friction. A special concave vibration envelope is identified, validated by experiments and shown as a characteristic form of vibrations for digitally controlled systems with dry friction.

Keywords

digital position control, friction effects, stability

[1] Department of Mechatronics, Optics and Mechanical Engineering Informatics, Faculty of Mechanical Engineering, Budapest University of Technology and Economics, H-1521 Budapest, Hungary

[2] MTA-BME, Research Group on Dynamics of Machines and Vehicles, H-1521 Budapest, Hungary

[3] Department of Mechanical Engineering, McGill University, 817 Sherbrooke Street West, Montreal, Quebec, Canada, H3A 0C3

[*] Corresponding author, e-mail: budaicsaba@mogi.bme.hu

1 Introduction

Positioning is a basic task in robotics, where the applied controller aims to drive the robot into a desired position. Industrial robotic applications often demand for high accuracy, strict repeatability and at the same time, fast operation. Modern robots are equipped with digital motion controllers. The performance of these with respect to the above requirements are limited by the sampled data nature[1] of the applied digital control. For example, the positioning accuracy of a PD controller can be improved by the proportional control gain [1], but at the same time the system becomes less robust to parameter variations and might get unstable for large gain values [2]. The effect of sampling have been investigated in the literature in detail [2-6].

Reference [2] introduces tools and design methods for digitally controlled robots, [3-5] focus on the analytical investigation of the dynamics of digital force control and [6] presents also experiments that show how sampling and quantization can cause performance limitations. In these studies the effect of Coulomb friction is considered as a stabilizing effect and it is neglected. This provides sufficffient conservativism in many cases in the control design, but cannot be applied when dry friction is the dominant or the only source of physical dissipation.

It is possible to derive an equivalent viscous damping to represent Coulomb friction by using the method of describing function analysis [7, 8]. To simplify the analysis and reduce computational costs, it is usual to model the dissipative forces due to the actuators, the motion transmission elements and bearings as viscous damping [9]. Structural damping is often considered in the form of modal damping. This type of viscous damping often captures well the combined effect of different dissipation mechanisms, and as it will be shown later in the paper, it can also be successfully applied to model friction effects in digitally controlled systems. However, in certain parameter ranges viscous damping alone cannot explain the experimentally observed decaying of vibrations.

1 Temporal and spatial discretization including time delays in data acquisition and processing.

Coulomb friction is shown to be stabilizing small, micro-chaotic motions caused by digital control [10-12]. Other work that analysed the possibly chaotic motion of systems with dry friction include [13-16]. By modelling the actual contact interfaces friction models get complicated. Such models are often used in feed forward friction compensation of robots [9, 17-19] assuming continuous time control. Still how the friction effects influence the stability of digital position control is not well understood, and left without discussion in the specialist literature.

In this paper we present a detailed analysis how Coulomb friction is influencing the stability properties of systems subjected to digital position control. This is illustrated by the example of a digitally controlled pendulum. First a mechanical model is developed in Section 2 which includes the non-linear effect of velocity reversals, and considers the temporal discretization due to sampling. Then, a detailed simulation study is conducted in Section 3 and the results are compared with the analytical results obtained for the undamped/frictionless case. The results are verified by experiments in Section 4, and Section 5 summarizes and concludes the paper.

2 Mechanical model

2.1 Piecewise continuous model

To illustrate the effect of Coulomb friction in digital position control we consider a single link, pendulum-like, direct drive robot (Fig. 4) operating around its stable equilibrium position. It is further assumed that only a simple proportional (P) controller is applied where the continuous time control input is realized by a zero-order-hold and has a unit delay. With these considerations the governing equation of motion of the system can be written as

$$\begin{aligned} I\ddot{\varphi}(t)+k_t\varphi(t)+C\,\mathrm{sign}\left(\dot{\varphi}(t)\right)=-k_p\varphi\left(t_{j-1}\right),\\ t\in\left[t_j,\ t_{j+1}\right),\quad t_j=j\Delta t,\quad j=0,1,2\ldots, \end{aligned} \tag{1}$$

where I denotes the mass moment of inertia with respect to the pivot joint, k_t is the effective torsional stiffness due to gravity and C is the magnitude of the dry friction torque. In addition, k_p is the proportional gain, Δt is the sampling time, t_j denotes the j-th sampling instant and $\varphi(t_{j-1})$ is the sampled and delayed control input.

2.2 Discrete switched model

In order to obtain a discrete time model for the stability analysis in a compact form we introduce the dimensionless time $T = \omega_n t$ with $\omega_n = \sqrt{k_t/I}$ denoting the natural angular frequency of the uncontrolled system. With this the dimensionless sampling instants become $T_j = j\Delta T = j\omega_n\Delta t$, and based on Eq. (1) we can obtain

$$\begin{aligned} \varphi''(T)+\varphi(T)+f_0\,\mathrm{sign}\left(\varphi'(T)\right)=-p\varphi_{j-1},\\ T\in\left[T_j,\ T_{j+1}\right), \end{aligned} \tag{2}$$

where $f_0 = C/k_t$, $\varphi_{j-1} = \varphi(T_{j-1})$ and $p = k_p/k_t$ is the dimensionless gain. In addition, symbol prime denotes differentiation with respect to the dimensionless time, i.e. $\varphi'(T) = \mathrm{d}\varphi(T)/\mathrm{d}T = 1/\omega_n\dot{\varphi}(t)$.

By assuming that the direction of motion does not change the piecewise linear equation of motion Eq. (2) can be solved in closed form for the consecutive sampling instants for the dimensionless discrete state variables collected in $\mathbf{z}_j = \left[\varphi_j \quad \dot{\varphi}_j \quad \varphi_{j-1}\right]^{\mathrm{T}}$; and the following discrete mappings can be derived

$$\mathbf{z}_{j+1} = \begin{cases} \mathbf{A}\mathbf{z}_j + \mathbf{a}, & \varphi'(T) < 0 \\ \mathbf{A}\mathbf{z}_j - \mathbf{a}, & \varphi'(T) < 0 \end{cases}, \tag{3}$$

with

$$\mathbf{A} = \begin{bmatrix} \cos(\Delta T) & \sin(\Delta T) & p\left(\cos(\Delta T)-1\right) \\ -\sin(\Delta T) & \cos(\Delta T) & -p\sin(\Delta T) \\ 1 & 0 & 0 \end{bmatrix},$$

$$\mathbf{a} = \begin{bmatrix} f_0\left(1-\cos(\Delta T)\right) \\ f_0\sin(\Delta T) \\ 0 \end{bmatrix}.$$

These mappings can form the basis of further numerical stability analysis, where the intersample velocity reversals has to be taken also into consideration. When the sampling time is sufficiently small compared to the period of oscillation of the system, however, Eq. (3) can directly be used for approximate discrete time simulation.

Beside the physical properties, the simulated dynamic behaviour depend on two control parameters: the dimensionless proportional gain p and the dimensionless sampling time ΔT. For the appropriate choice of them, the stable domain of the operation has to be determined.

3 Stability analysis

3.1 Stability neglecting friction

First we investigate the case when Coulomb friction is neglected. The corresponding result can serve as a reference to examine the effect of friction on system stability. In this case Eq. (3) becomes $\mathbf{z}_{j+1} = \mathbf{A}\mathbf{z}_j$. Using this linear map, the time series of the dimensionless discrete state variables can be determined for any initial condition. These states form a multi-dimensional geometric series [2], therefore the system is asymptotically stable if and only if, the spectral radius of the state transition matrix, $\rho(\mathbf{A})$, is less then unity. For the eigenvalues of $\mathbf{A}$ this is equivalent to the condition $|\mu_i| < 1$, $i = 1, 2, 3$ [20].

We note that this condition can further be analysed by using the Moebius transformation $\mu = (\eta + 1)/(\eta - 1)$, and applying the Routh-Hurwitz stability criteria. With this the stability boundaries can be obtained in closed form as it is explained in [2]. The stable domain of control parameters is illustrated

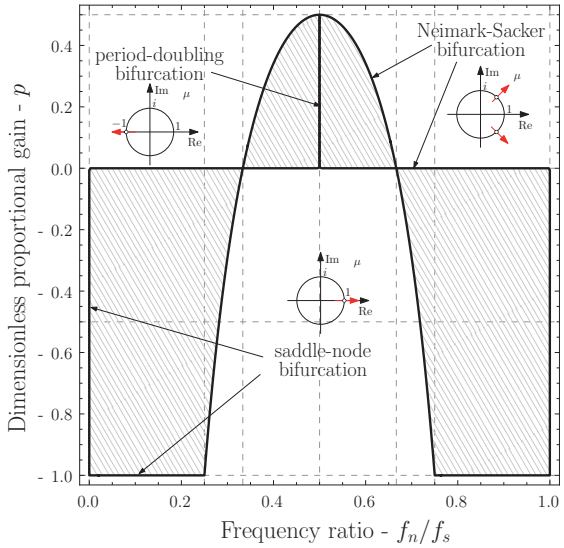

Fig. 1 Stability chart

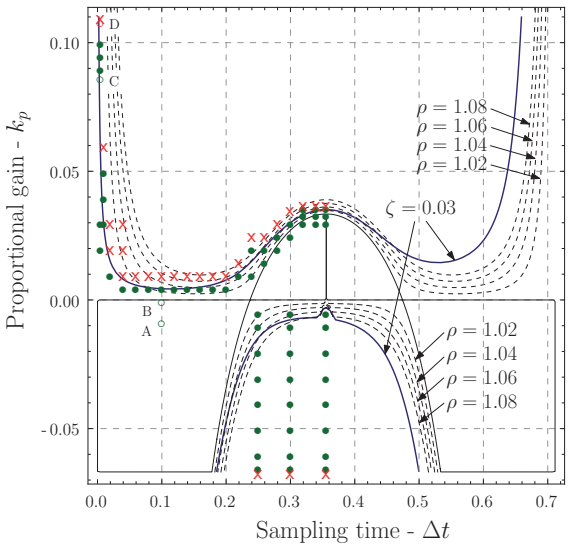

Fig. 2 Stability with dry friction/damping

in the plane of frequency ratio f_n/f_s and dimensionless proportional gain p in Fig. 1, where $f_n = \omega_n/2\pi$ and $f_s = 1/\Delta t$ are the natural and sampling frequencies of the system respectively. The solid black contour represents the stability boundary, where the spectral radius $\rho(\mathbf{A}) = 1$, and the grey hatched area is the stable domain of the control parameters.

As for the pendulum gravity creates a constant effective stiffness, the position control problem investigated above can also be interpreted as a special force control with zero desired force and proportional feedback $-\tilde{k}_p k_t \varphi_{j-1}$, where $\tilde{k}_p$ is the dimensionless force feedback gain. Based on this, it can be shown that the stability chart in Fig. 1 is the same as the one presented in our previous work [4,5]. For further details on stability properties the reader is referred to this publication.

It has to be also mentioned, that the presented stability chart in Fig. 1 is periodic in the frequency ratio with periodicity 1, and it is not necessary to have small sampling times to achieve stable position control. However, there are practical limitations. According to Shannon's sampling theorem the frequency ratio f_n/f_s should be less than 1/2, where $f_N = f_s/2$ is the Nyquist frequency [22] and $f_n \leq f_N$ is required. When this is not satisfied, aliasing (frequency folding) may occur. This phenomenon does not influence the stability of the system, but typically leads to "noisy" system responses with superimposed high-frequency oscillations.

3.2 Stability with friction

When friction is not neglected Eq. (3) forms a switched, non-homogeneous discrete mapping, where velocity reversals can also occur between two sampling instants. Therefore the same analysis as in Section 3.1 cannot be used. For specific system parameters where the dominant vibration period[2] is an integer multiple of the sampling time it might still be possible to create a homogeneous mapping that can further be investigated to check system stability. In general, however, it is not possible, and here we will use numeric simulation to show the effect of Coulomb friction. The analytical approach outlined above is left for future work.

For the practically important frequency ratios, the results of our simulation study are collected in Fig. 2. Here the thin black lines give the contour of the stable domain, and the dashed black lines are associated with different spectral radii in the domain which would be unstable without friction. The solid blue line represents the stability boundary when viscous damping is considered with a realistic damping ratio. The green and red bullets show the stable and unstable simulations, respectively, where the stability of certain special solutions (sticking states) were determined based on the detection of decreasing/increasing amplitudes of the simulated vibrations. In addition, the empty red and green circles labelled with letters show the simulation parameters whose time histories are also presented in Fig. 3. These results were obtained by using the 4-th order Runge-Kutta scheme for the integration with fixed time-step $h = \Delta t/100$ and considering the initial conditions $\varphi(0) = 0.2325$ rad and $\dot{\varphi}(0) = 0$ rad/s. The mechanical and control parameters used in these simulations are collected in Table 1 and 2 and the model of the investigated pendulum system is described in detail later in Section 4.2).

During simulation we observed that friction did not influence the saddle-node type stability boundaries. The stable domain was expanded along the boundaries where the system were originally losing its stability with vibrations, and the previously stable domains (see Fig. 1) remain stable. Figure 2 shows that small friction can stabilize the system with control parameters selected from the lower region, $f_n/f_s \leq 1/2$ and $0 > k_p > -k_t$, of the stability chart. At small sampling times the same amount of friction drastically increase stability and

2 Vibration associated with the pair of complex eigenvalues having the largest magnitude.

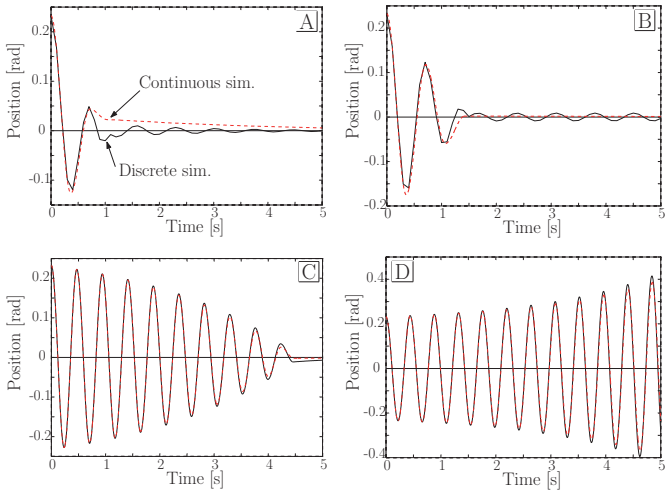

Fig. 3 Typical time-histories of vibrations

Table 1 Control parameters for simulation

A	Δt	100	ms	k_p	−8.4	mNm/rad
B	Δt	100	ms	k_p	0*	mNm/rad
C	Δt	5	ms	k_p	87.7	mNm/rad
D	Δt	5	ms	k_p	108.3	mNm/rad

* The controller is switched off

makes it possible to select large gain values in positioning. For larger sampling times (e.g., $0.1 < \Delta t < 0.35$) the effect of friction on the upper stability boundary is less apparent, it mainly contributes to the robustness of the P controller designed without considering friction.

In many cases, only viscous damping is used to model dissipation and Coulomb friction is neglected. To compare the effect of viscous damping with the above results, a small damping ratio $\zeta = 0.03$ was considered in the model which neglects friction. The damping ratio was chosen to approximate the simulation results with friction. In Figure 2 it can be seen, that in the upper part of the stability chart the stability boundaries corresponding to the different dissipation models are in good agreement. But in the lower region of the stability chart we can observe a major difference. Here the system is mostly unstable with viscous damping, while Coulomb friction stabilizes all the possible vibrations. Reference [21] presents experimental results that validate our simulations corresponding to higher k_p values, but no results are provided for negative k_p values. It is probable that instabilities could not be experimentally measured in that region due to the effect of dry friction.

We also note that, the equivalent viscous damping obtained by describing function analysis [8] depend on the initial conditions. When this is not taken into account during experiments, measurement results might become inconsistent as they might belong to different effective viscous damping values.

The typical dynamic behaviours of position controlled mechanical systems with Coulomb friction is summarized in

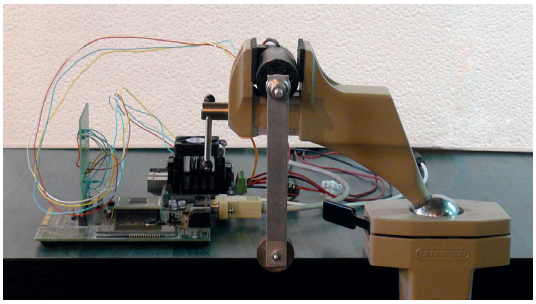

Fig. 4 Experimental setup

Fig. 3, where the time-histories corresponding to parameter settings A, B, C and D defined in Fig. 2 and Table 1 are plotted. Panel A shows the time-history of a simulation which would be stable without friction. In this case, the physical dissipation due to friction makes the transient shorter, but a larger positioning error is expected. The vibrations shown in panel B correspond to the uncontrolled system. The control parameters are chosen from the Neimark-Sacker type stability boundary, where following the initial linear decaying of the vibration amplitudes, sustained oscillations develop. The results presented in panel C are very typical to mechanical systems with dry friction and often observed in experiments. Here the dissipation effect of Coulomb friction counteracts the destabilizing effects of sampling and special vibrations can be observed with a concave envelope. The presence of this type of vibrations is a clear indication to that the dissipation mechanism is dominated by Coulomb friction. When the proportional gain is increased too much in order to reduce the positioning error, instability might occur. This is illustrated in panel D.

4 Experimental validation

4.1 Experimental setup

The investigated experimental setup is a brushed DC motor (Maxon A-max 32, 236670) driven pendulum using a self-developed control board (see Fig. 4). This consists of a low-level controller using a PIC (24FJ128GA010) microcontroller which communicates with a Simulink Real-Time Workshop based high-level controller via RS-232 communication protocol. The pendulum is connected directly to the brushed DC motor shaft.

The microcontroller processes the measured data from the encoder of the DC motor, and transmits the calculated angle to the PC. The Simulink model calculates the required control torque, and transmits it in the form of a PWM signal to an H-bridge through the microcontroller.

Table 2 Effective model and control parameters

U_0	12	V	J_r	44	gcm²
R	7.17	Ω	J_p	8.569	kgcm²
k_m	46.1	mNm/A	k_t	66.84	mNm/rad
i_0	32.2	mA	b_t	0.296	mNms/rad
r_m	794	-	C	1.925	mNm

4.2 Model of experimental setup

As the magnitude of the mechanical time constant is two times greater than the magnitude of electric time constant of the used DC motor, the inductance of the motor can be neglected. With this assumptions the equation of motion of a DC motor is

$$\frac{k_m}{R}\left(u_{in}(t)-k_m\dot{\varphi}(t)\right)=J_r\ddot{\varphi}(t)+\tau_f(t)+\tau_l(t), \qquad (4)$$

where u_{in} is the input voltage, R denotes the terminal resistance, k_m is the motor torque constant, J_r is the mass moment of inertia of the rotor. In addition φ, $\dot{\varphi}$ and $\ddot{\varphi}$ are the angular position, velocity and acceleration of the DC motor shaft, respectively, τ_f denotes the friction torque and τ_l is the external load.

During the experiments the pendulum was commanded to maintain its vertical, hanging-down equilibrium position. Considering also its direct drive actuation the load is $\tau_l = J_p\ddot{\varphi} + k_t\varphi$, where J_p is the mass moment of inertia of the pendulum about the motor shaft, k_t is the torsional stiffness due to gravity, and φ is measured from the equilibrium.

The friction torque can be determined as $\tau_f = C\ \mathrm{sign}(\dot{\varphi})$ assuming Coulomb friction, and it can initially be approximated[3] as $C = k_m i_0 = 1.4844$mNm, where i_0 is the no load current. This value is in good agreement with our experiments where the pendulum typically stopped in the range of 1−2 degrees corresponding to $C = 1.2$−2.5 mNm. For the further calculations we select $C = 1.925$ mNm which value gives the best matching results with the experiments.

Plugging the load τ_l into Eq. (4) the equation of motion of the experimental system can be given in the form

$$J\ddot{\varphi}(t)+b_t\dot{\varphi}(t)+k_t\varphi(t)+C\ \mathrm{sign}\left(\dot{\varphi}(t)\right)=\tau_{in}(t), \qquad (5)$$

where the input torque $\tau_{in} = k_m u_{in}/R$, $b_t = k_m^2/R$ is the effective torsional viscous damping due to the motor back EMF and $J = J_r + J_p$ is the effective mass moment of inertia. The system parameters are collected in Table 2.

We note that the effect of Coulomb friction was dominant over viscous damping in our experiments. The uncontrolled system clearly has a linear vibration envelope even when the amplifier was connected, but τ_{in} was set to zero.

The unit delay considered previously in Eq. (1) models the fact that the Simulink model transmits the output force first, and processes the received input later in the same control cycle. With this the input torque can be expressed as

$$\tau_{in}(t) = -k_p\varphi(t_{j-1}) = \frac{k_m U_0}{R}\frac{\hat{k}_p\phi(t_{j-1})}{r_m}, \qquad (6)$$

where U_0 is the nominal voltage of the DC motor, ϕ denotes the angular position in encoder counts, and r_m is the maximum duty cycle resulting from the applied PWM frequency and the efficiency of the H-bridge.

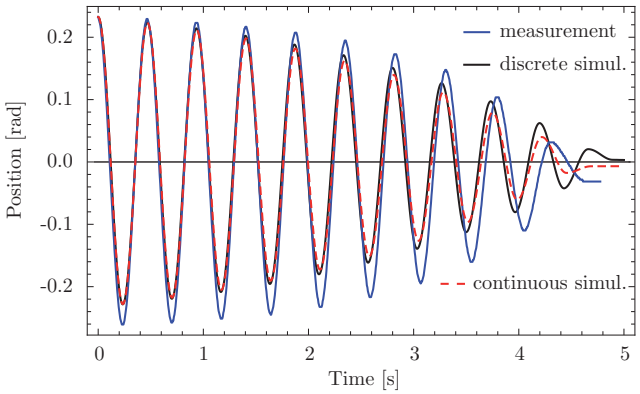

Fig. 5 Simulation vs. experimental results

4.3 Effect of Coulomb friction

In this section we present experimental results that validate the simulation corresponding to point C in Fig. 2 and Fig. 3. At this point the results show a concave vibration envelope which is characteristic to digitally controlled systems with friction.

The measured and simulated time history are shown together in Fig. 5. The experimental results are shown in blue, the solid black line corresponds to the simulation with discrete mapping in Eq. (3) by disregarding the inter-sample velocity reversals, and the red curve was obtained with the continuous time model in Eq. (1). All the results are in good agreement with the experiments and all of them have concave vibration envelopes. The larger errors in the amplitudes in the negative direction are due to the asymmetric friction properties of the experimental device. This is not included in the model and can be seen as a possibility for future improvements.

5 Conclusion

In this study the effect of Coulomb friction on the dynamics of digitally controlled mechanical systems was investigated through the analysis of the effective model of the experimental setup of a digitally controlled pendulum. It was shown where Coulomb friction stabilizes the otherwise unstable motion, the damped vibrations have a concave envelope. This is characteristic to digitally controlled systems with dry friction.

The effect of friction on system stability was also analysed in an extensive set of simulations and the results were presented on the stability chart obtained analytically for different models. Compared with modal (or effective viscous) damping dry friction has a similar stabilization effect for positive gain values, but a significant difference was observed for negative k_p values. In this region dry friction completely stabilizes the system, while viscous damping gives only slight stability improvements. The presented stability results and the simulation based dynamic analysis are verified by experiments.

3 The friction torque can depend on the contact force in general, and therefore will slightly vary as the pendulum rotates with different speeds.

Acknowledgement

This work was supported by the MTA-BME Research Group on Dynamics of Machines and Vehicles. The support is gratefully acknowledged.

References

[1] Asada, H., Slotine, J. J. E. "*Robot Analysis and Control*." Wiley, New York, 1986.

[2] Stepan, G., Steven, A., Maunder, L. "Design principles of digitally controlled robots." *Mechanism and Machine Theory*. 25 (5). pp. 515-527. 1990. DOI: 10.1016/0094-114X(90)90066-S

[3] Stepan, G. "Vibrations of Machines Subjected to Digital Force Control." *International Journal of Solids and Structures*. 38 (10-13). pp. 2149-2159. 2001. DOI: 10.1016/S0020-7683(00)00158-X

[4] Kövecses, J., Kovacs, L. L., Stepan, G. "Dynamics modeling and stability of robotic systems with discrete-time force control." *Archive of Applied Mechanics*. 77 (5). pp. 293-299. 2007. DOI: 10.1007/s00419-006-0085-x

[5] Kovacs, L. L., Kövecses, J., Stepan, G. "Analysis of effects of differential gain on dynamic stability of digital force control." *International Journal of Non-Linear Mechanics*. 43 (6). pp. 514-520, 2008. DOI: 10.1016/j.ijnonlinmec.2008.04.002

[6] Budai, Cs., Kovacs, L. L. "Limitations Caused by Sampling and Quantization in Position Control of a Single Axis Robot." In: *Proceedings of the XV. International PhD Workshop*. Wisla, Poland, pp. 466-471, Oct. 2013.

[7] Townsend, W., Salisbury, J. "The effect of Coulomb friction and stiction on force control." In: *Proceedings of the IEEE International Conference on Robotics and Automation*, Raleigh, North Carolina, USA, pp. 883-889, March. 1987. DOI: 10.1109/ROBOT.1987.1087936

[8] Haas, V. B. "Coulomb friction in feedback control systems." *Transactions of the American Institute of Electrical Engineers, Part II: Applications and Industry*. 72 (2). pp. 119-126. 1953. DOI: 10.1109/TAI.1953.6371269

[9] Armstrong-Helouvry, B., Dupont, P., Canudas de Wit, C. "A survey of models, analysis tools and compensation methods for the control of machines with friction." *Automatica*. 30 (7). pp. 1083-1138. 1994. DOI: 10.1016/0005-1098(94)90209-7

[10] Enikov, E., Stepan, G. "Microchaotic Motion of Digitally Controlled Machines." *Journal of Vibration and Control*. 4 (4). pp. 427-443. 1998. DOI: 10.1177/107754639800400405

[11] Csernak, G., Stepan, G. "Digital control as source of chaotic behavior." *International Journal of Bifurcation and Chaos*. 20 (5). pp. 1365-1378. 2010. DOI: 10.1142/S0218127410026538

[12] Gyebroszki, G., Csernak, G., Budai, Cs. "Experimental investigation of micro-chaos." In: *Proceedings of 8th European Nonlinear Dynamics Conference*, Vienna, Austria, pp. 1-6, July. 2014.

[13] Den Hartog, J. P. "Forced vibrations with combined Coulomb and viscous friction." *Transactions of the American Society of Mechanical Engineers*. 53. pp. 107-115. 1931.

[14] Shaw, S. W. "On the dynamic response of a system with dry friction." *Journal of Sound and Vibration*. 108 (2). pp. 305-325. 1986. DOI: 10.1016/S0022-460X(86)80058-X

[15] Fenny, B., Moon, F. C. "Chaos in a forced dry friction oscillator: experiment and numerical modelling." *Journal of Sound and Vibration*. 170 (3). pp. 303-323. 1994. DOI: 10.1006/jsvi.1994.1065

[16] Csernak, G., Stepan, G. "On the periodic response of a harmonically excited dry friction oscillator." *Journal of Sound and Vibration*. 295 (3-5). pp. 649-658. 2006. DOI: 10.1016/j.jsv.2006.01.030

[17] Canudas de Wit, C., Olsson, H., Astrom, K. J., Lischinsky, P. "A new model for control of systems with friction." *IEEE Transactions on Automatic Control*. 40 (3). pp. 419-425. 1995. DOI: 10.1109/9.376053

[18] Olsson, H., Åström, K. J., Canudas de Wit, C., Gäfvert, M., Lischinsky, P. "Friction models and friction compensation." *European Journal of Control*. 4 (3). pp. 176-195. 1998. DOI: 10.1016/S0947-3580(98)70113-X

[19] Dupont, P., Armstrong-Helouvry, B., Hayward, V. "Elasto-plastic friction model: Contact compliance and stiction." In: *Proceedings of the American control conference*, Chicago, Illinois, USA, pp. 1072-1077, 2000. DOI: 10.1109/ACC.2000.876665

[20] Kuo, B. C. "*Digital Control Systems*." SRL Publishing, 1977.

[21] Kisfalusi, K., Stréli, T., Stepan, G. "Experimental study of digital force control." Proceedings in Applied Mathematics and Mechanics. 5 (1). pp. 167-168. 2005. DOI: 10.1002/pamm.200510063

[22] Åström, K. J., Wittenmark, B. "C*omputer Controlled Systems: Theory and Design*." Prentice Hall, Upper Saddle River, N.J., 2nd edition, 1990.